

# X-ray and electron diffraction study of penfieldite: average structure and multiple cells

S. MERLINO, M. PASERO, N. PERCHIAZZI

Dipartimento di Scienze della Terra, Università di Pisa, Via S. Maria 53, I-56126 Pisa, Italy

AND

A. GIANFAGNA

Dipartimento di Scienze della Terra, Università di Roma 'La Sapienza', P. le A. Moro 5, I-00185, Roma, Italy

## Abstract

Penfieldite is a lead hydroxychloride mineral with composition  $\text{Pb}_2\text{Cl}_3(\text{OH})$ . It belongs to the hexagonal system, space group  $P\bar{6}$ ,  $a = 11.393(3)$ ,  $c = 4.024(1)$  Å. The 4 Å  $c$  parameter corresponds to the basic sub-cell, whereas modulated structures are known with a true  $c$  axis 12 times longer. The average crystal structure of penfieldite has been solved with direct methods and refined to  $R_w = 0.041$  for 871 reflections collected with Mo- $K\alpha$  radiation. The chemical and structural relationships between penfieldite and laurelite,  $\text{Pb}_2\text{F}_3(\text{F}, \text{Cl}, \text{OH})$ , are briefly discussed. An electron diffraction study of penfieldite revealed the occurrence, besides the common modulated structure with  $C = 12c$ , of domains with a  $15c$  periodicity. Moreover, a  $9c$  periodicity has been observed in crystals heated at 180°C. Penfieldite is quickly destroyed above 200°C.

KEYWORDS: penfieldite, lead halides, crystal structure, laurelite, modulated structures, TEM.

## Introduction

PENFIELDITE is a rare lead hydroxychloride mineral, first described from Laurion, Greece, by Genth (1892). In that paper the mineral was assigned to the hexagonal system, and the chemical formula  $\text{Pb}_3\text{Cl}_4\text{O}$  was proposed. Penfield (1894) presented morphological data, whereas optical data were reported by Larsen (1917). Later on, penfieldite was found at Sierra Gorda, Chile (Gordon, 1941), and on two Roman anchors in the Mediterranean Sea, the former found in front of Mahédia, Tunisia, the latter near the Îlot des Formigues, Var, France (Goni *et al.*, 1954). Gordon (1941) provided detailed morphological data for penfieldite from Laurion and from Sierra Gorda, giving for the former specimen the chemical formula  $\text{Pb}_2\text{Cl}_3(\text{OH})$  and a measured density of 6.61 g/cm<sup>3</sup>. Markedly different density values, 5.86 and 5.82 g/cm<sup>3</sup>, which better match the theoretical value, were reported thereafter by Palache

*et al.* (1951) and by Cesbron and Schubnel (1968), respectively.

X-ray data for penfieldite were first reported by Goni *et al.* (1954), who presented the powder patterns for penfieldite from Laurion and from Îlot des Formigues. A more detailed X-ray study of penfieldite was carried out by Cesbron and Schubnel (1968), who obtained Weissenberg photographs for both samples from Laurion and Sierra Gorda. The latter authors indicated the Laue symmetry  $6/m$ , with  $a = 11.28(3)$ ,  $c = 48.65(8)$  Å, and present a new powder pattern of the mineral, somewhat different with respect to the previous data (Goni *et al.*, 1954).

More recently, penfieldite was discovered in the Etruscan iron slags of Baratti beach, near Piombino, Tuscany, Italy (Franzini and Perchiazzi, 1992), together with 41 other species, mainly copper and/or lead oxy- and hydroxychlorides, sulphates and carbonates. It occurs as small (up to 1 mm in length) hexagonal prisms (Fig. 1), sometimes associated with

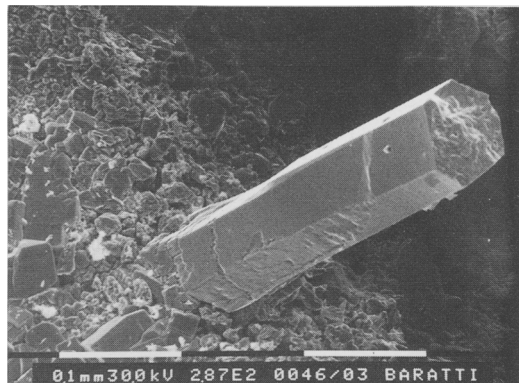


FIG. 1. SEM photograph of a well developed crystal of penfieldite from Baratti. Scale bar = 0.1 mm.

fiedlerite,  $\text{Pb}_3\text{Cl}_4\text{F}(\text{OH})\cdot\text{H}_2\text{O}$  (Merlino *et al.*, 1994), and rarely with cotunnite,  $\text{PbCl}_2$ . We undertook the study of penfieldite from this new locality, together with samples from the type locality and from Sierra Gorda, with the aim of getting a deeper insight into the structural and microstructural features of the mineral.

A microprobe analysis (average of three points) on penfieldite from Baratti (ARL/SEMQ wavelength-dispersion electron microprobe, working conditions 15 kV, 10 nA, beam diameter 10  $\mu\text{m}$ , standards: metallic Pb for Pb, sodalite for Cl, synthetic  $\text{CaF}_2$  for F, and matlockite,  $\text{PbClF}$ , for all three elements) gave the following results: Pb 78.41%, Cl 19.31, F 0.09 (O 3.30, H 0.21), leading to the chemical formula  $\text{Pb}_2\text{Cl}_{2.88}\text{F}_{0.03}(\text{OH})_{1.09}$ .

#### X-ray data

A number of penfieldite crystals from Baratti, Laurion and Sierra Gorda were studied by Weissenberg and precession methods. A peculiar feature in the reciprocal lattice of the mineral, already observed by Cesbron and Schubnel (1968), is the presence of strong and populated reciprocal lattice layers with  $l = 12n$ , which define a subcell with  $c \approx 4 \text{ \AA}$ , and very weak additional reflections with  $l = 12n \pm 1$ . All other reflections are almost extinct.

The powder pattern of penfieldite from Baratti (Table 1) is identical in all strongest lines to that given for a sample from Laurion by Goni *et al.* (1954), differing only in a number of additional weak to very weak reflections in the low- $d$  region. We would remark that all foreign reflections reported by Cesbron and Schubnel (1968) in the high- $d$  region, i.e. reflections which cannot be indexed on the basis of the  $c \approx 4 \text{ \AA}$  subcell, are probably due to another

TABLE 1. Powder pattern of penfieldite from Baratti (Gandolfi camera, 114.6 mm in diameter,  $\text{Cu-K}\alpha$  radiation). Indexing was made with the help of the single crystal intensity data collection

$l$	$d_{\text{meas}}$	$d_{\text{calc}}$	$hkl$
w	9.88	9.87	100
m	5.66	5.696	110
mw	4.901	4.933	200
S	3.714	3.729	120
m	3.282	3.287	111
mS	3.177	3.118	201
vw	2.805	2.848	220
m	2.732	2.735	211
m	2.538	2.547	301
mw	2.456	2.467	400
mw	2.327	2.325	221
mS	2.263	2.263	311
m	2.150	2.153	410
vw	2.105	2.103	401
m	1.975	1.973	500
mw	1.902	1.899	330
m	1.864	1.865	240
mw	1.620	1.622	340
vw	1.578	1.622	151
vw	1.521	1.580	520
vw	1.521	1.522	601
mw	1.504	1.505	160
m	1.473	1.470	412
mw	1.419	1.410	350
mw	1.419	1.409	611
mw	1.369	1.368	242
w	1.343	1.343	441
vw	1.331	1.330	531
mw	1.296	1.296	261
mw	1.264	1.263	450
vw	1.244	1.263	342
vw	1.234	—	—
w	1.206	—	—
mw	1.156	—	—

phase. In fact their interplanar spacings correspond to those of most of the strongest peaks of fiedlerite, and it seems inappropriate to index them as superstructure ( $l \neq 12n$ ) reflections of penfieldite, as it happens on the JCPDS card no. 22-384.

#### Structure analysis

The crystal structure analysis of penfieldite was undertaken on the basis of the subcell with  $c \approx 4 \text{ \AA}$ , owing to the substantial lack of measurable reflections with  $l \neq 12n$ . This suggested that the structure of penfieldite was characterized by

TABLE 2. Final fractional coordinates and  $B$  equivalent isotropic thermal parameters for penfieldite

Atom	$x$	$y$	$z$	$B_{eq}$
Pb1	0.6221(1)	0.5386(1)	$\frac{1}{2}$	1.21(4)
Pb2	0.1743(1)	0.2739(1)	0	1.15(4)
Cl1	0.8564(7)	0.8059(7)	$\frac{1}{2}$	0.9(2)
Cl2	0.8272(8)	0.5324(8)	0	1.4(3)
Cl3	0.3212(8)	0.4683(8)	$\frac{1}{2}$	1.3(2)
O	0.590(2)	0.652(2)	0	1.0(7)

modulations along [001] of a basic layer. The intensity data collection was carried out with a single crystal of penfieldite from Baratti (dimensions  $0.1 \times 0.2 \times 0.5$  mm) using an Ital Structures four-circle automatic diffractometer, equipped with graphite-monochromatized Mo- $K\alpha$  radiation ( $\lambda = 0.71069$  Å) and working at 48 kV and 28 mA. The collection was performed in  $\omega$ - $2\theta$  scan mode, scan width in  $\theta \pm (0.8^\circ + 0.15^\circ \tan \theta)$ ,  $2\theta_{max} = 60^\circ$ , scan speed 1.5 to 6.5°/min, depending on the intensity of a pre-scan of the peaks. Two standard reflections (410 and 002) were monitored at 3 h intervals, and showed intensity variations within  $\pm 2\sigma$ . The unit cell parameters  $a = 11.393(3)$  Å,  $c = 4.024(1)$  were obtained through least-squares fit of  $2\theta$  values of 24 reflections ( $20^\circ < 2\theta < 30^\circ$ ). All measured intensities were reduced for Lorentz and polarization factors. The Laue symmetry and the lack of systematic absences pointed to  $P6$ ,  $P\bar{6}$  and  $P6/m$  as possible space groups. Therefore direct methods (SHELXS86; Sheldrick, 1986) were applied in all three cases. A

reliable E-map, revealing the positions of the two independent Pb atoms, was obtained in the  $P\bar{6}$  space group only. Chlorine and oxygen atoms were then localized through alternating Fourier syntheses calculations and least-squares refinement cycles (SHELX76; Sheldrick, 1976). After an empirical correction for the absorption effects (DIFABS; Walker and Stuart, 1984; correction factors on  $F$  in the range 0.80–1.24;  $R_{symm}$  from merging equivalents 0.036 and 0.024 before and after the correction, respectively), the refinement was completed using anisotropic thermal parameters, and a weighting scheme based on  $w = 1/[\sigma(F_o)]^2$ , to  $R = 0.049$ ,  $Rw = 0.041$  for 871 independent reflections. The oxygen atom displays a strongly elongated thermal ellipsoid. Such a physically meaningless feature could probably depend on minor inaccuracies in the absorption correction. Neutral atomic scattering factors  $f$ ,  $f'$ ,  $f''$  were taken from the International Tables for X-ray Crystallography (1974). The final fractional coordinates and equivalent isotropic displacement parameters are given in Table 2. A supplementary table with the observed and calculated structure factors is available from the editor.

### Description of the structure

A picture of the structure of penfieldite in terms of lead coordination polyhedra is presented in Fig. 2, whereas bond distances are reported in Table 3.

All the atoms in the structure of penfieldite lie on symmetry planes at either  $z = 0$  or  $z = \frac{1}{2}$ . The two independent lead atoms, Pb1 and Pb2, are linked to eight anions in a bicapped trigonal prismatic configuration. However, the two coordinations do not match between each other, either from the chemical or from the geometrical point of view. In

TABLE 3. Selected interatomic distances (Å) in penfieldite. Distances marked with an asterisk occur twice

Pb1	– Cl2	(*)	3.111(8)	Pb2	– Cl1	(*)	3.002(5)
	– Cl2	(*)	3.158(6)		– Cl1	(*)	3.339(7)
	– O	(*)	2.514(16)		– Cl3	(*)	2.837(5)
	– Cl1		2.876(6)		– Cl2		3.229(10)
	– Cl3		3.106(9)		– O		2.456(28)
Cl2	– Cl2	(*)	3.61(1)	Cl1	– Cl1	(*)	3.44(1)
O	– Cl2	(*)	3.58(2)	Cl3	– Cl1	(*)	3.99(1)
O	– Cl2	(*)	3.58(3)	Cl3	– Cl1	(*)	4.23(1)
Cl1	– Cl2	(*)	3.58(1)	Cl2	– Cl1	(*)	3.58(1)
Cl1	– O	(*)	3.32(2)	Cl2	– Cl3	(*)	3.75(1)
Cl3	– Cl2	(*)	3.75(1)	O	– Cl1	(*)	3.32(2)
Cl3	– O	(*)	3.38(2)	O	– Cl3	(*)	3.35(2)
Cl2	– Cl2	(*)	4.024(1)	Cl1	– Cl1	(*)	4.024(1)
O	– O		4.024(1)	Cl3	– Cl3		4.024(1)

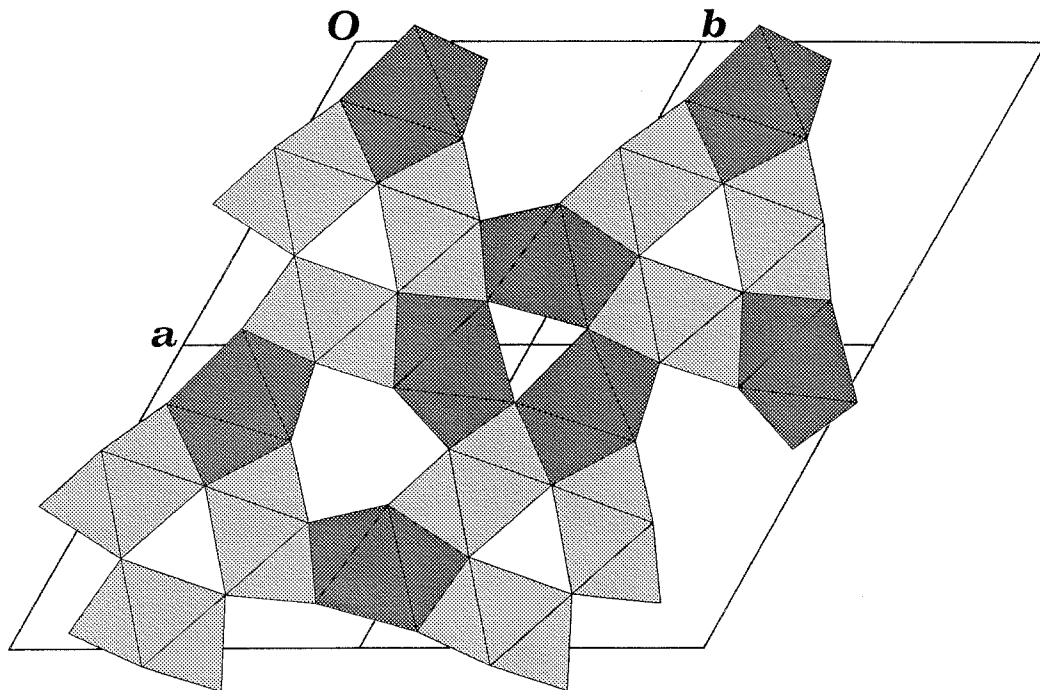


FIG. 2. The crystal structure of penfieldite, as seen in [001] projection in terms of lead coordination polyhedra. Lower and higher shadings represent Pb1- and Pb2-centred polyhedra, respectively.

fact Pb1 is surrounded by 6 Cl + 2 (OH), whereas Pb2 is surrounded by 7 Cl + 1 (OH). Moreover, the bases of the Pb1-centred prisms are almost perfect equilateral triangles, those of the Pb2-centred prisms are severely distorted triangles.

A look at the positions of the coordinating anions around Pb reveals that they can be divided in two pairs, Cl3 and (OH), and Cl1 and Cl2, which play balanced crystal-chemical roles in Pb1- and Pb2-centred polyhedra. In fact Cl3 and (OH), as well as Cl1 and Cl2, act alternately as capping anion and bases of the prism (Fig. 3).

If we consider the coordinations of the chlorines, we can observe that Cl1 and Cl2 display nearly identical coordinations: in fact both are connected to 5 Pb atoms in a square pyramidal configuration. Contrarily, Cl3 atoms are differently coordinated, being linked to three Pb atoms only. The resulting bond valence deficiency for Cl3 could be balanced by O—H...Cl hydrogen bonding. In fact the O atom displays two O—Cl3 approaches of 3.35(2) and 3.38(2) Å. The oxygen atom can be considered as lying at the centre of a tetrahedron having three Pb atoms at three corners, with an hydrogen atom placed in the direction of the fourth corner. This seems just the right direction for an O—H...Cl bond. Because of

the presence of the heavy atoms, it is obviously impossible to reveal the actual position of the hydrogen atoms. As O and Cl lie on symmetry planes displaced by  $c/2$ , the O—H...Cl bonds could be of either of the following two kinds: (1) The H atom too lies on the same symmetry plane as the O, and a bifurcated O—H < Cl hydrogen bond with two Cl atoms lying on two neighbouring planes, above and below the O—H plane, occurs. Such hydrogen bonding is not uncommon (Hamilton and Ibers, 1968), and has been recently described in the crystal structure of paralaurionite, another lead hydroxychloride with formula PbCl(OH) (Merlino *et al.*, 1993); (2) The hydrogen atom leaves the plane moving towards either of the two chlorines, resulting in a simple O—H...Cl bond. This would lower the space group symmetry from  $P6$  to  $P3$ , although the higher symmetry could be the result of a statistical distribution of simple upwards- and downwards-pointing O—H...Cl bonds.

#### Relationships with laurelite

Laurelite is a newly discovered mineral, described by Kampf *et al.* (1989) from the Grand Reef mine, Arizona, USA. Close relationships between laurelite

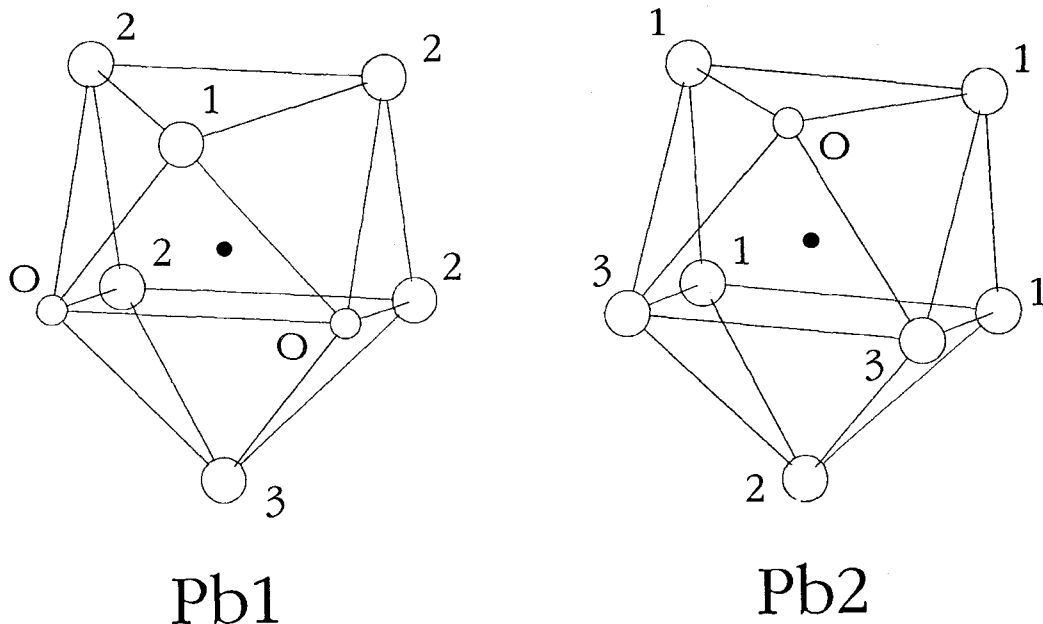


FIG. 3. The two independent lead coordination polyhedra, described as bicapped trigonal prisms. Central lead atoms are indicated by the small filled circles. 1, 2, 3, and O denote Cl1, Cl2, Cl3 and the oxygen belonging to the (OH) group, respectively.

and penfieldite may be hypothesized, on the basis of the similarities in both the chemical composition and the unit cell parameters. In fact the chemical formula of laurelite may be written as  $Pb_2F_3(F,Cl,OH)$ , which closely matches that of penfieldite, with fluorine playing the same role as chlorine, and with three different anions statistically distributed within the same structural site. Laurelite is hexagonal, Laue class  $6/m$ , with  $a = 10.252(9)$ ,  $c = 3.973(1)$  Å. The decrease of the  $a$  parameter, with respect to penfieldite, is related to the lower dimensions of the  $F^-$  anions if compared with those of  $Cl^-$ . The shortening is not so pronounced for the  $c$  parameter, which mainly depends on the  $Pb \cdots Pb$  interactions between lead atoms at  $(x, y, z)$  and  $(x, y, 1+z)$ . Moreover, a close correspondence has been observed between the indices of the strongest lines of the powder patterns for the two minerals.

As for now, we do not know whether modulated structures occur in laurelite, too, even if it should be probable. A single-crystal structural analysis of the mineral is at present in progress (Kampf, pers. comm.). Hopefully, a combined investigation of penfieldite and laurelite by X-ray and electron diffraction could provide a better comprehension of the fine structural details of both minerals.

### TEM study

A transmission electron microscopy study of penfieldite was undertaken, with the aim of collecting more detailed information on the nature of the superlattice reflections. The TEM study was carried out with samples of penfieldite from Baratti and from Laurion, and gave similar results in both cases. All of the photographs presented in this work were taken on penfieldite from Baratti. A Philips 400T electron microscope was used (operating conditions: standard hairpin tungsten filament, accelerating voltage 120 kV, beam current in the range 20–50  $\mu A$ ). Penfieldite has proven to be highly unstable under the electron beam, and in normal condition its structural features are completely lost in a few seconds. It was, therefore, impossible to obtain any direct lattice image (Fig. 4). Some electron diffraction photographs were taken, working with undersaturated filament and with an under- or overfocused beam, and, on reaching normal beam current values, focusing only for the time necessary to take the photograph.

Bearing in mind that Cesbron and Schubnel (1968) observed, on X-ray [001] rotation photographs, very weak diffraction effects which defined a periodicity

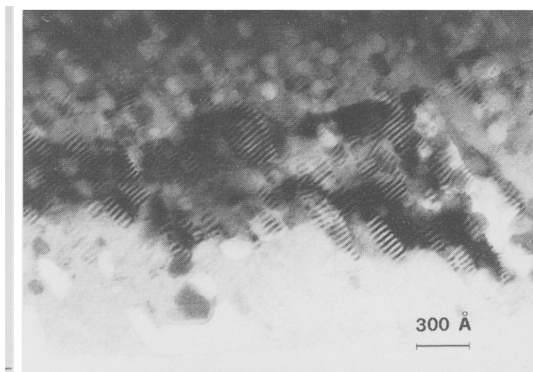


FIG. 4. Transmission electron micrograph of penfieldite, featuring conspicuous damages due to the electron beam.

$C = 12c \approx 48 \text{ \AA}$ , we obtained a number of SAED patterns which contained the  $\mathbf{c}^*$  vector. Indeed, the  $C = 12c$  periodicity represents a very common feature in penfieldite from both Baratti and Laurion, even at the submicroscopic scale. Cesbron and Schubnel (1968) observed sharp spots with  $l = 12n$  (corresponding to the subcell with  $c \approx 4 \text{ \AA}$ ) and weak spots with  $l = 12n \pm 1$ . In our electron diffraction patterns, additional spots with  $l = 12n \pm 2$  are also present (Fig. 5). The intensities of the superstructure reflections, as normally happens with electron diffractions, are higher than those obtained with X-rays.

Besides the common patterns which correspond to a superstructure with  $C = 12c$ , other diffractions were found which define a periodicity  $C = 15c \approx 60 \text{ \AA}$  (Fig. 6). In these SAED patterns the diffraction effects of the subcell have  $l = 15n$ , additional diffractions have  $l = 15n \pm 1, \pm 2, \pm 3$ . The modulation of the intensities along the  $\mathbf{c}^*$  direction is typical.

In some cases we observed, from the same crystal fragment, a transition from the periodicity with  $C = 15c$  to the periodicity with  $C = 12c$ . As an hypothesis, it seems reliable to relate the variation of the modulation with the moderate heating of the crystals under working conditions into the TEM instrument.

To test this hypothesis, we performed X-ray diffraction rotation photographs on crystals of penfieldite heated within a furnace at different temperatures. Preliminary data indicate that penfieldite decomposes above  $200^\circ\text{C}$ . Moreover, another interesting feature has been observed, namely a transition in the modulated periodicity from  $C = 12c$  to  $C = 9c \approx 36 \text{ \AA}$ , in a crystal of penfieldite from Baratti heated at  $180^\circ\text{C}$  for 15 min. Such a periodicity was not observed in our electron

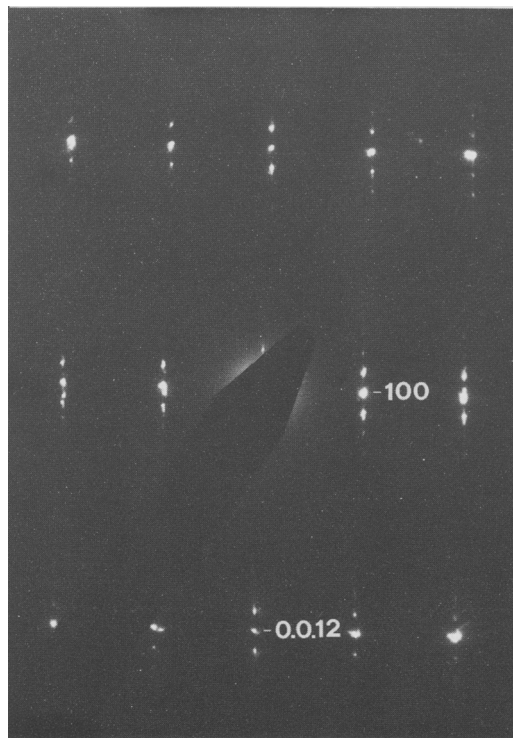


FIG. 5. Selected area electron diffraction of penfieldite. Zone axis [010]. The periodicity along  $\mathbf{c}^*$  corresponds to a  $12c \approx 48 \text{ \AA}$  parameter.

diffraction patterns, and could represent a metastable state during the heating. It is noteworthy that all superstructures so far observed are multiple of a  $3c \approx 12 \text{ \AA}$  period, which therefore could represent a basic module in all modulated structures. On progressive heating, penfieldite could rearrange itself, assuming different modulated structures ( $15c, 12c, 9c$ ) before it loses crystallinity above  $200^\circ\text{C}$ . Penfieldite therefore appears, from a thermodynamic point of view, as a mineral phase with a low stability region, in which different modulated structures could represent the result of subtle equilibria between energetic and entropic terms. Edwards *et al.* (1992), who tried unsuccessfully to synthesize penfieldite, suggest that it is metastable.

Unfortunately, the lack of high resolution lattice images prevents us from putting forward any reliable hypothesis on the microstructural arrangements in penfieldite. Tentatively, the modulation phenomena could be related to concerted ordering of the hydrogen bonds along [001], associated with minor distortions of the structure. To verify it, further data are needed.

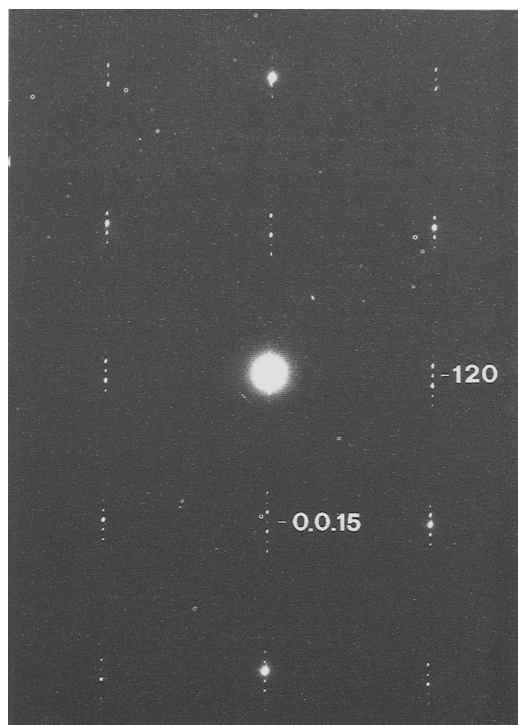


FIG. 6. Selected area electron diffraction of penfieldite. Zone axis  $[210]$ . The periodicity along  $c^*$  corresponds to a  $15c \approx 60 \text{ \AA}$  parameter.

### Acknowledgements

We are indebted to P. J. Dunn (Smithsonian Institution, Washington) for the specimen no. R9109 of penfieldite from Sierra Gorda; to A. R. Kampf (Natural History Museum, Los Angeles) for a specimen of laurelite; and to Ch. Rewitzer (Furth-im-Wald), for a specimen of penfieldite from Laurion. G. Vezzalini (University of Modena) is thanked for performing the microprobe analyses. Financial support by MURST (40% grant to S. Merlino) is acknowledged.

### References

- Cesbron, F. and Schubnel, H. J. (1968) Nouvelles données sur la penfieldite. *Bull. Soc. Fr. Minéral. Cristallogr.*, **91**, 407–8.  
 Edwards, R., Gillard, R. D., Williams, P. A. and Pollard, A. M. (1992) Studies of secondary mineral formation

- in the  $\text{PbO-H}_2\text{O-HCl}$  system. *Mineral. Mag.*, **56**, 53–65.  
 Franzini, M. and Perchiazzi, N. (1992) I minerali delle scorie ferrifere etrusche di Baratti (Livorno). *Atti Soc. Tosc. Sc. Nat., Ser. A*, **99**, 43–77.  
 Genth, F. A. (1892) On penfieldite, a new species. *Amer. J. Sci.*, **44**, 260.  
 Goni, J., Guillemin, C. and Perrimond-Tronchet, R. (1954) Description d'espèces minérales néogènes formées sur des jas d'ancres romaines immergées. *Bull. Soc. Fr. Minéral. Cristallogr.*, **77**, 474–8.  
 Gordon, S. G. (1941) Results of the Chilean mineralogical expedition of 1938. Part III — Penfieldite from Sierra Gorda, Chile. *Not. Nat. Acad. Nat. Sci. Philadelphia*, **69**, 1–8.  
 Hamilton, W. C. and Ibers, J. A. (1968) *Hydrogen Bonds in Solids*. W. A. Benjamin, Inc., New York, 284 pp.  
 International Tables for X-ray Crystallography (1974) Vol. IV, J. A. Ibers and W. C. Hamilton (eds), The Kynock Press, Birmingham, 362 pp.  
 Kampf, A. R., Dunn, P. J. and Foord, E. E. (1989) Grandreefite, pseudograndreefite, laurelite and aravapaite: four new minerals from the Grand Reef mine, Graham County, Arizona. *Amer. Mineral.*, **74**, 927–33.  
 Larsen, E. S. (1917) The optical properties of penfieldite. *Amer. Mineral.*, **2**, 20.  
 Merlino, S., Pasero, M. and Perchiazzi, N. (1993) Crystal structure of paralaurionite and its OD relationships with laurionite. *Mineral. Mag.*, **57**, 323–8.  
 Merlino, S., Pasero, M. and Perchiazzi, N. (1994) Fiedlerite: revised chemical formula  $[\text{Pb}_3\text{Cl}_4\text{F}(\text{OH})\cdot\text{H}_2\text{O}]$ , OD description and crystal structure refinement of the two MDO polytypes. *Mineral. Mag.*, **58**, 69–78.  
 Palache, C., Berman, H. and Frondel, C. (1951) *Dana's System of Mineralogy, Vol. II*. J. Wiley and Sons, Inc., New York, 7th ed., 1124 pp.  
 Penfield, S. L. (1894) Mineralogical notes. *Amer. J. Sci.*, **48**, 114–8.  
 Sheldrick, G. M. (1976) *SHELX76 — Program for crystal structure determination*. Univ. of Cambridge, England.  
 Sheldrick, G. M. (1986) *SHELXS86 — Program for the solution of crystal structures*. Univ. of Göttingen, Germany.  
 Walker, N. and Stuart, D. (1984) An empirical method for correcting diffractometer data for absorption effects. *Acta Crystallogr.*, **A39**, 158–66.  
 [Manuscript received 7 May 1993; accepted 18 November 1994]